Astron. Astrophys. 296, 761–770 (1995)

ASTRONOMY AND ASTROPHYSICS

Decoupled line driven outflow around B and Be stars

John M. Porter and Janet E. Drew

Department of Physics, Nuclear and Astrophysics Lab., Keble Road, Oxford OX1 3RH, UK

Received 13 May 1994 / Accepted 23 August 1994

Abstract. The semi-analytic model of Bjorkman & Cassinelli for the equatorial 'discs' around Be stars is re-examined and shown to be capable of producing higher equator-to-pole density contrasts when the effects of the dynamical decoupling of the stellar radiation field from the outflowing gas are incorporated. The enhancement, as measured by the normal component of the momentum fed into the disc, is in the region of a factor of 2. Inclusion of the effect also lowers the threshold stellar rotation rate for the formation of a wind-compressed disc from $v_{rot}/v_{crit} \simeq 0.4$ to 0.25.

Two physical mechanisms that may give rise to this decoupling, which are most effective in B star winds, are presented and their relative merits compared. This comparison is performed with reference to available UV and X-ray observations. Ion-stripping (Springmann & Pauldrach 1992) could be the cause of the low observed maximum outflow velocities, but it cannot simultaneously explain the ubiquitous high-temperature ($\gtrsim 10^6$ K) X-ray emission. Shock disruption of the wind ionization balance (Castor 1987) may also terminate the outward radiative acceleration in the winds of B stars. This effect suggests a simple method for setting an upper limit to the X-ray emission from weak shock-disrupted winds which compares reasonably favourably with X-ray luminosities derived from ROSAT data.

Key words: stars: emission-line, Be – stars: mass-loss – ultraviolet: stars – X-rays: stars

1. Introduction

The geometry of Be star envelopes has been argued to be non-spherically symmetric from contrasts between the UV and optical/IR line profiles. The C IV 1549Å and Si IV 1397Å UV line profiles provide evidence of high velocity outflows, similar to the fast flowing ($v \sim$ 1000-3000 km s^{-1}) winds associated with O stars. The origin and main features of these wind-formed profiles in normal O stars are well understood in the context of radiation driven wind theory (Castor et al. 1975; Friend & Abbott 1986; Kudritzki et al. 1986). By contrast, the optical and IR hydrogen lines in Be star spectra are in emission, with much lower characteristic velocities of a few hundred kilometers per second. Models of equatorial discs have been used to good effect in interpreting this emission (Pockert & Marlborough 1978) and also the IRAS excesses derived for these stars (Cotè & Waters 1987; Waters et al. 1987).

Whilst this two component model of the Be star envelope has been very successful as a phenomenological model, attributing much higher densities to the equatorial outflow, it leaves unanswered the question of the physical origin of the circumstellar 'disc'. Until recently the best candidate for the cause of this structure was non-radial pulsation (e.g. Willson 1986; Ando 1991). There is now an appealing alternative to consider in the mechanism proposed by Bjorkman & Cassinelli (1993) that is expected to produce strong equatorial focusing of the radiation-driven winds from rapidly-rotating B stars. In such stars, it is the centrifugal force rather than radiation pressure that is the wind's main support against gravity during its initial acceleration away from the stellar photosphere. The motion of a fluid element may thus contain a significant rotational component which, together with a weaker radial component, will define an orbital plane that in general is inclined to the star's equatorial plane. Gas rotating in these angled planes must pass through the star's equatorial plane. In cases where many such streamlines cross the equator, the result is focusing of the outflow into what has been termed a wind compression disc (WCD). Thus, a combination of initially small radial and high rotational velocities can result in mass loss from a substantial fraction of the stellar surface being driven toward the stellar equator.

Bjorkman & Cassinelli predict that their model will produce equator to pole density ratios of $\sim$ 800. Owocki et al. (1994) have reported that $2\frac{1}{2}$D numerical hydrodynamical simulations of WCDs achieve almost, but not quite the density contrast predicted from Bjorkman & Cassinelli's model – they find this ratio to be $\sim$300–600 for a range of stellar rotation rates. Estimation of this ratio from observation is uncertain to perhaps as much as an order of magnitude. The polar density is obtained from combining the UV mass loss rates (Snow 1981) with the mass continuity constraint, while the equatorial density must be derived from fits to IR excesses (Waters et al. 1987). Calculated in this way, ratios in the region of a few 10^4 are obtained. Hence it seems that not all the ingredients needed to fit the Bjorkman

& Cassinelli mechanism to the Be star case have yet been identified.

In this paper, we consider two physical effects, that will raise the equator-to-pole density contrast. Both effects operate by truncating the line force in the supersonic part of the flow. This further enhances the effect of rotation. One of these effects is ion stripping (Dreicer 1959, 1960) and the other is that of disruption of the wind ionization balance through shocking (Castor 1987; Abbott & Friend 1989). As both these mechanisms have most impact in low density flows they may have a significant rôle to play in B star winds.

The rest of this paper is arranged as follows: firstly the two mechanisms are examined (Sect. 2) and decoupling radii are derived. Then, in Sect. 3 the decoupling radii are calculated for a sample of stars. A model star is then used in deriving the wind structure using Bjorkman and Cassinelli's prescription in Sect. 4. Observational implications of this effect are then summarized in Sect. 5.

2. Decoupling mechanisms

2.1. Ion stripping

The mechanism by which ionic runaway may be achieved was first discussed by Dreicer (1959, 1960), in the context of electrical conductivity. Its relevance to OB star winds has been examined by Springmann & Pauldrach (1992), and also by Gayley & Owocki (1994) whose concern is primarily with the energy balance.

In OB stars, the radiation force is mediated primarily by scattering of photons in lines of heavy element ions. These ions then share their momentum with the major mass component of hydrogen and helium ions (henceforth referred to as the plasma) via a process, akin to friction, whose effectiveness depends on the mean drift velocity w_D between the driven ions and the plasma. At low drift velocities, the interaction cross section is proportional to w_D/a_P, where a_P is the thermal velocity of the protons, ($a_P^2 = [2kT/m_P]$; k is the Boltzmann constant, T is the gas temperature, and m_P is the mass of a proton). In this regime, a close coupling between the ions and plasma is maintained, enabling the bulk flow of the gas. The cross section increases with the drift velocity until it reaches a maximum at $A_{ip}w_D^2/a_P^2 = 1$ (A_{ip} is the reduced mass of the ions and the plasma). Further increase in the drift velocity beyond this value causes a reduction in the cross section (at high w_D, it decreases as $[w_D/a_P]^{-2}$). Should a line-driven wind enter this regime, decoupling of the driven ions from the plasma soon follows, cutting off the bulk of the gas from further acceleration – the effect of interest here. Beyond the decoupling radius, the vanishing frictional force exposes the ions to sharp acceleration that strips them out of the plasma. Detection of the driven ions can then be assumed to be practically impossible as their density must decrease precipitously.

For the present purpose, we require an expression for the radius at which ion-stripping may be expected to occur. A 'beta' velocity law of the form

$$v = v_\infty(1 - R_*/r)^\beta, \tag{1}$$

is assumed to apply for radii less than the decoupling radius. This is an acceptable approximation, even for outflow disrupted by radiation-driven instability, in that the 1D hydrodynamic simulations by Owocki et al. (1988) supports the idea that the mean flow still adheres to the steady flow solution. Hence, the major concern is rather to choose values of β and v_∞ consistent with modified CAK theory.

The terminal velocity v_∞ is that derived for a fully coupled wind according to the following expression from Friend & Abbott (1986):

$$v_\infty = \frac{2.2\alpha}{1-\alpha} v_{esc} \left(1 - \sin(\theta)\frac{v_{rot}}{v_{crit}}\right)^{0.35}. \tag{2}$$

Here θ is the angle between the polar axis and the radial steamline considered ($\theta = 0$ at the pole, $\theta = \pi/2$ at the equator), α is the Castor et al. (1975) index applied to the optical depth term in the force multiplier. The escape velocity v_{esc} is defined by $v_{esc} = \sqrt{2GM_*(1-\Gamma_e)/R_*}$, where $M_*$and $R_*$are the stellar mass and radius respectively. The critical rotational velocity v_{crit}, is that for breakup, $v_{crit} = v_{esc}/\sqrt{2}$. Γ_e is the ratio of the force due to Thomson scattering to gravity.

The ratio of the line force to gravity, Γ_L, may be expressed as a function of radius for a fully coupled wind, and compared with the radial dependence of this ratio imposed by the requirement that the ion drift velocity be equal to its critical value (where $A_{ip}w_D^2/a_P^2 = 1$). The radius at which these two expressions are equal defines the decoupling radius, r_I. Springmann & Pauldrach (1992) and also Gayley & Owocki (1994) obtain

$$\frac{\beta\, v_{\infty\,3}^3\, (1 - R_*/r_I)^{3\beta-1}\, T_4\, R_*}{\dot{M}_{-9}} = 1.5 \times 10^3\, Y_i\, Z_i^2\, \ln\Lambda, \tag{3}$$

where $v_{\infty\,3} \equiv v_\infty/10^3$ km s^{-1}, and the stellar radius is expressed in solar units. Also Y_i is the mass fraction of the ions, Z_i is the degree of ionization, and $\dot{M}_{-9} \equiv \dot{M}/10^{-9}\mathrm{M}_\odot\,\mathrm{yr}^{-1}$is the mass loss rate derived from UV line profiles. T_4 is the temperature of the gas in units of 10^4K. The decoupling radius r_I, is then

$$r_I = R_* \left\{ 1 - \left(\frac{1.5 \times 10^3\, Y_i\, Z_i^2\, \ln\Lambda\, \dot{M}_{-9}}{\beta\, v_{\infty\,3}^3\, T_4\, R_*} \right)^{\frac{1}{3\beta-1}} \right\}^{-1}. \tag{4}$$

The constants used in this expression are: $Y_i \sim 1.5 \times 10^{-3}$, $Z_i \sim 3$, representing triply ionized driving ions. The Coulomb logarithm $\ln(\Lambda) \sim 20$ for interstellar material. The radiation driving parameters (Abbott 1982; Friend & Abbott 1986; Pauldrach et al. 1986) used here are $\alpha = 0.55 \pm 0.05$, $k = 0.15 \pm 0.05$, $\delta \sim 0.1$ and $\beta = 0.8$.

From Eq. (3), ion stripping will be most likely to occur in winds of low mass loss rate and high terminal velocity. Winds of the appropriate character have been detected around B and Be stars; mass loss rates are typically $\sim 10^{-9}$–$10^{-10}\mathrm{M}_{\odot}\,\mathrm{yr}^{-1}$ (Snow 1981) and velocities $v_{\infty} \sim 1000 - 2000$ km s^{-1} from Eq. (2).

Note that the terminal velocity used here, v_{∞}, cannot be reached if decoupling of the ions and plasma occurs at a finite radius. Its significance in decoupled winds is that of a scaling parameter, fixing the magnitude of the velocity derivative inside the decoupling radius. Note also that v_{∞} is calculated from Eq. (2) and is *not* the maximum outflow velocity derived from line profiles, which may be much less (Grady et al. 1987).

An alternative, and more accurate, description is obtained when then internal energy of the outflow is calculated. The gas may be heated by the frictional interaction (Mauche & Raymond 1987; Springmann & Pauldrach 1992; Gayley & Owocki 1994), increasing the temperature of the gas, making ionic runaway more likely. As the drift velocity increases, the frictional heating increases (the heating rate is proportional to w_D). The heating of the gas leads to lower frictional cross sections and hence to higher drift velocities. This thermally-induced ion stripping produces decoupling radii closer to the star than those predicted from Eq. (4).

The flow is heated by the frictional interaction, and cooled mainly by line radiation, adiabatic expansion and recombination. Using the 'beta' velocity law, and its associated density structure, the temperature may be calculated by manipulating the equation of energy conservation to give:

$$\partial_r T = -\frac{2}{3}\left(\frac{2}{r} - \frac{\partial_r v}{v}\right) T + \frac{2Q^{rad}}{3kv} + \frac{2H\partial_r v}{3k} T, \qquad (5)$$

where ∂_r denotes differentiation with respect to the radius r. H is a constant containing v_{∞}, $\dot{M}$ and β. The first term on the right hand side is the adiabatic cooling, the second contains a radiative cooling term taken from Raymond et al. (1976), and the third represents the frictional heating. From the temperature, the frictional cross section is calculated. This through the fluid equations yields the drift velocity and, again using $A_{ip}w_D^2/a_P^2 = 1$ as a decoupling criteria, the ion stripping radius r_I can be derived. The radius r_I derived from this thermally induced runaway is significantly less than that derived from Eq. (4), using a purely dynamical argument. For the representative Be star used later in Sect. 4, we find that with no rotation $r_I \simeq 1.1R_*$ for thermally induced decoupling, whereas $r_I \simeq 2.0R_*$ for the dynamical calculation.

From the point of view of calculation of the velocity law, the region over which ion stripping occurs is treated as infinitely thin – no account of partial decoupling has been taken. In fact it can be argued that this is quite a good approximation. The firm expectation is that the length-scale involved for each ionic species will be very short - again using the representative Be star in Sect. 4 as an example, we find that for the ionic species which produce most radiative acceleration (SiIII, FeIII, CIII and CII - see Table 5 from Abbott 1982), $A_{ip}w_D^2/a_P^2$ increases from 0.5 to 1.0 in $\sim 0.01R_*$. However, different ionic species decouple at different radii - we find that the range over which the ionic species contributing most acceleration decouple is from $1.07R_*$ for CII and FeIII to $1.17R_*$ for CIII. On passing through this region, the outflow recieves progressively less acceleration than a fully coupled wind. Despite this, Abbott & Friend (1989) have shown that the velocity law still truncates almost instantaneously at a mean cut-off radius. Indeed, their Fig. 2 shows that the truncation of the fully coupled velocity law is very abrupt even in the case that the line force is cut off over a range of $\sim 0.4R_*$ (their model with s = 10), four times our estimate of the cut-off width.

2.2. Shock decoupling

Radiatively driven winds have been understood to be susceptible to the growth of instabilities for many years now (Lucy & Solomon 1970; MacGregor et al. 1979; Owocki & Rybicki 1984). Once a small scale perturbation forms in a radiation-driven wind, it may quickly steepen to form a shock (Owocki et al. 1988). The observable consequences of this are, in some instances, non-thermal radio emission (Abbott et al. 1981, 1984), and more commonly X-ray emission (Harnden et al. 1979; Cassinelli et al. 1994). Analyses of X-ray observations of OB stars have yielded shock temperatures in the range $\sim 10^6 - 10^7$ K (Cassinelli & Swank 1983; Chlebowski et al. 1989; Drew et al. 1994).

Wind shocking has also been identified as the possible cause of the unexpectedly low terminal velocities of late O and early B main sequence stars (e.g. Abbott & Friend 1989). The shocking itself *and* the X-rays emitted ionize the gas locally. Indeed, in low density winds the effects of X-ray ionization can penetrate a significant distance upstream. Certainly, at low mass loss rates, the gas downstream cannot cool and the ionization state of the shocked gas will remain out of equilibrium, thus preventing the resumption of significant line driving (Castor 1987). The wind then coasts. Provided these effects do not alter conditions at the hydrodynamic critical radius, the mass loss rate is unchanged.

For the case of strong shocks, Krolik & Raymond (1985) present a critical column density N_c below which the gas cannot cool *radiatively* to recover its pre-shock ionization state: $N_c \sim 7 \times 10^{21} v_{j\,3}^4\,\mathrm{cm}^{-2}$, where $v_{j\,3}$ is the velocity jump across the shock, in units of 10^3 km s^{-1}. The temperature of the post-shock gas is $T_s = 1.4 \times 10^7 v_{j\,3}^2 K$. Together these yield

$$N_c \sim 3.6 \times 10^{19} \left(\frac{T_s}{10^6\mathrm{K}}\right)^2 \mathrm{cm}^{-2}. \qquad (6)$$

The remaining wind column density N beyond a shock at r_S is given by

$$N = \int_{r_S}^{\infty} n_e dr, \qquad (7)$$

where n_e is the electron density. The density of the wind at r_S is obtained from the continuity equation $\rho = \dot{M} / 4\pi r_S^2 v_S$. In the case that the gas does not cool and recombine, the postshock velocity of the wind v_S remains approximately constant at $v_S = v(r_S)$ outside the decoupling radius r_S. With $n_e = \rho/\mu_e m_H$

(μ_e is the mean molecular weight per electron, and m_H is the mass of a proton) the limiting column density may be written

$$N = \frac{\dot{M}}{4\pi\mu_e m_H r_S v_S}. \tag{8}$$

We now need an estimate for the postshock velocity v_S and the shock radius r_S. For those stars whose winds plausably pass through a decoupling shock, we can measure the maximum blueshifted velocity, v_{edge}, of the absorption components of wind formed lines (Grady et al.1987). This corresponds to the maximum velocity attained by the cool wind. In strong adiabatic shocks, the postshock velocity of the gas is a quarter of the preshock velocity, in the shock's rest frame. Therefore, the postshock velocity v_S could be in principle be as low as $v_S = v_{edge}/4$. In view of the character of shocks in OB star winds (see simulations be OCR), we can expect the unperturbed velocity given in Eq. 1 to lie between v_{edge} and v_S. Furthermore, there is no reason to expect the shock structure to be coherent over large solid angles about the star. Hence to calculate the critical column density we need a suitable average of the product of the postshock velocity and the shock radius $< v_S r_S >$ (averaged over time and over the whole star). For want of a better choice we proceed with the assumption that the velocity law of Eq. (1) provides a reasonable estimate of r_S for a given v_S. The postshock velocity will be some fraction of the edge velocity, $v_S = \xi v_{edge}$, where $1 \leq \xi \leq 0.25$. Using this the the product of postshock velocity and decoupling radius may be written

$$< v_S r_S >= R_* v_\infty \left(\frac{(\xi v_{edge}/v_\infty)}{1 - (\xi v_{edge} v_\infty)^{1/\beta}} \right). \tag{9}$$

Equating the two expressions for column density (Eqs. 6 and 8), allows the critical shock temperature T_S to be determined if $\dot{M}$ is known. The appropriate expression is:

$$\frac{T_S}{10^6\mathrm{K}} = 3.22 \left[\left(\frac{\dot{M}}{10^{-9} M_* \,\mathrm{yr}^{-1}} \right) \left(\frac{1 - (\xi v_{edge}/v_\infty)^{1/\beta}}{R_*} \right) \left(\frac{v_\infty}{1000\mathrm{km\,s}^{-1}} \right)^{-1} \left(\frac{\xi v_{edge}}{v_\infty} \right)^{-1} \right]^{1/2} \mathrm{K}. \tag{10}$$

Accordingly, our expression for $T_S(\dot{M})$ is sensitive to assumptions about ξ - the shock structure. However, the error produced here is typically similar to the uncertainty in the mass loss rate derived from ultraviolet line profile fitting.

This prescription, is similar to that used by Abbott & Friend (1989), and has also been tried out for the case $\xi = 1$ by Drew et al. (1993) in their study of the mass loss rates for β and ϵ CMa. It is encouraging to note that this treatment provided an estimate of the mass loss rate for β CMa that is consistent with the value derived by Kudritzki et al. (1991) from UV line profile fitting.

Knowledge of this parameter ξ and the mass loss rate $\dot{M}$ can be turned into an upper limit on the expected X-ray emission. To do this, it is assumed that it takes just one significant shock to terminate the cool equilibrium phase of a B star wind. An integration over the volume of emission of the product of the cooling function and density squared requires the temperature structure to be specified. However, given the uncertainties already discussed in the shock temperature prescription, we adopt a simpler approach which will provide a reasonable estimate. We assume that all the energy in the postshock gas, $C_v T_S(\dot{M})$ is converted into radiation. This then produces an upper limit to the total emission. The limiting luminosity L_X emitted is

$$\begin{aligned} L_X &\leq \zeta(T_S(\dot{M}))\dot{M} C_v T_S \\ &\propto \zeta(T_S(\dot{M}))\dot{M}^{3/2} \end{aligned} \tag{11}$$

where C_v is the specific heat, and $\zeta(T_S(\dot{M}))$ is the fraction of luminosity produced by the shock in the X-ray waveband. This correction is as low as ~ 0.1 for a temperature of 0.5×10^6K, and rises to ~ 0.5 for 2×10^6K. A luminosity above this limit can be allowed if (i) the terminating shock is the last of a train of shocks (as envisaged in the model of Lucy 1982, for instance), (ii) there is a quite separate source of X-rays present, such as the shocks at the surface of the WCD predicted in the Bjorkman & Cassinelli picture, (iii) the shock interpretation placed on the lower than expected maximum cool wind outflow velocities is simply wrong. Of course, there is no physical reason why the terminating shock temperature may not be higher than T_S. Equation (11) continues to define an upper limit even in this circumstance. This follows from the fact that the radiative cooling rate is a flat or decreasing function of temperature for $T \gtrsim 10^5 K$ (Gaetz & Salpeter 1983).

In effect, Eq. (11) is a prediction of a very simple model of B-star X-ray emission that can be compared with observation.

3. Observational basis

In order to determine the importance of the two mechanisms it is necessary to compare observational data with the analysis above. Key studies of the properties of fast winds of B and Be stars include Snow & Morton (1976), Snow (1981, 1982) and Grady et al. (1987). Here, two samples of B stars are examined: (i) a representative sample of stars with representative masses, radii, and temperatures for their spectral type, and (ii) a subset of the stars examined by Snow (1981). The comparison of the two samples serves to illustrate the extent of the uncertainties involved, which are considerable.

The stellar parameters are supplemented by the "edge" velocity of UV line profiles. Grady et al. (1987), have measured this velocity from IUE observations of 62 Be stars. It is defined as the apparent return to continuum at the short-wavelength edge of the line profile. Here, the edge velocity is interpreted to be the decoupling velocity of the wind of the last section.

For sample (i), mean values of the stellar parameters are taken from Underhill & Doazan (1982). The masses are derived from a sample of 71 main sequence stars in 45 binary systems given in *7th Catalogue of the Orbital Elements of Spectroscopic Binary Systems* (Batten et al. 1978). The quoted radii are due to Popper (1974, 1978), and the effective temperatures are from Underhill et al. (1979). The stellar parameters used here agree, within the errors below, with Schmidt-Kaler's (1982) compilation. Mass loss rates are derived from extrapolation of the fit to O star data due to Garmany et al. (1981). These are consistant to a factor of a few with mass loss rates derived from Kudritzki et al. 's (1989) "cooking recipe". As there seems to be a correlation between the edge velocities of the Be stars and escape velocity (see Fig. 8 of Grady et al. 1987), the decoupling velocities were evaluated from averaging the edge velocities in each spectral type. The properties of these representative stars are listed in Table 1, (nos. 1–7).

The data for sample (ii) (nos. 8–18 in Table 1) are based on the work of Snow (1981). He studied *Copernicus* observations for 21 B and Be stars. Mass loss rates were derived for all these stars by fitting theoretical profiles of the Castor & Lamers (1979) atlas to observed profiles. However, the individual stars' mass loss rates in many cases differ from the cooking recipe's predictions (Kudritzki et al. 1989), by up to a factor of ten. Masses, radii and effective temperatures for this sample are taken from representative values based on spectral type (Code et al. 1976). Only stars which have had edge velocities measured (from Grady et al. 1987) are included.

For both samples, the uncertainties are as follows: the masses are likely to be within 30% of their true values, the radii to within 10% , and the effective temperatures to within ±1500K (Popper 1974, 1978; Underhill & Doazan 1982).

The value of Snow's mass loss rates are influenced by the ionization balance assumed. The fraction of Si existing in SiV is unknown from the *Copernicus* data. It becomes dominant when SiIII /SiIV drops to 0.01 (Kallman 1980) although for the stars with both SiIII and SiIV observations this ratio does not fall below 0.01. Snow thus neglects SiV in his determination, which should only be important for the hottest stars in his sample. For this reason the earliest B stars in his sample have been omitted. For later types, Snow indicates that his derived mass loss rates are accurate to within a factor of a few (see Snow 1981 for more discussion).

3.1. Ion stripping and decoupling radii, and X-ray emission

The parameters above are now used to estimate decoupling radii and X-ray luminosities for both samples.

Beginning with the spectral type representative sample ((a) in Table 1), the ratio of the X-ray luminosity to bolometric luminosity is derived under the assumption of shock decoupling, using the formalism of 2.2. This ratio is plotted against spectral type in Fig. 1 and is listed in column 15 of Table 1. Cassinelli et al. 's (1994) ROSAT observations seem to indicate that X-ray luminosities decrease with spectral type. Happily, this trend is in keeping with the prediction (the solid lines in Fig. 1). The dominant factor in this trend as noted in Eq. (11) is the dependence on mass loss rate both directly and through $\zeta(T_S(\dot{M}))$. The dependence of the ratio on ξ at all spectral subtypes is less marked. To a first approximation we find that the simple prescription based on the concept of shock decoupling is not challenged by this limited set of measurements. Indeed it is encouraging to note that the observed luminosity ratios tend to lie at or below the estimated upper limits.

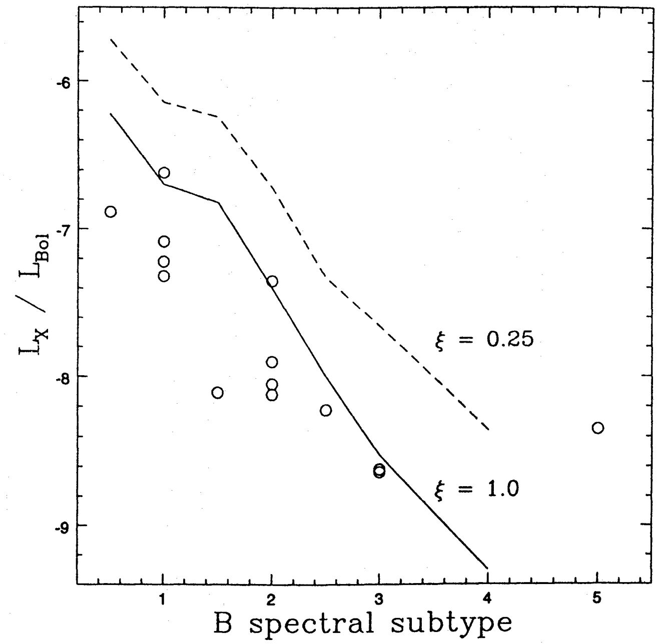

Fig. 1. Predicted X-ray luminosities vs. spectral type. The lines show the trend in the representative B stars for the two values of the parameter ξ (see text). The solid line corresponds to $\xi = 1.0$, and the dashed line to $\xi = 0.25$. These lines are the upper limits to the luminosity ratio. Open circles are the results of Cassinelli et al. 1994

However, whilst there is reason to suppose that the predicted trend in L_X/L_{Bol} is fairly secure, there is a problem in establishing its normalisation because of the uncertainties in B star mass loss rate determinations. To illustrate this we compare in Fig. 2 the ratios derived for the second sample of individual stars ((b) in Table 1) with those obtained from the representative sample ((a) in Table 1). Almost all the individual limits lie well below the curve drawn for the representative sample. A factor of ~3 decrease in the mass loss rates derived from extrapolation of Garmany et al. 's (1981) L_{Bol}-$\dot{M}$ relation is all that is needed to bring the representative B star sample (for $\xi = 0.25$) down amongst the majority of the ratios derived for the individual stars in the second sample, and also among the observations. As it happens, the extrapolated Garmany et al. relation was chosen for the representative sample because Snow (1982) indicated that it gave better agreement with his own semi-empirical mass loss rate estimates (Snow 1981) than any alternative then available. This was reassuring in that it compares favourably with the predictions of time-independent radiation driven wind theory (e.g. Friend & Abbott 1986). However, most of Snow's measurements actually lie below the extrapolated Garmany et al. relation (see Fig. 1 of Snow 1982), suggesting that the "true" mass loss rates for the representative B star sample are lower than quoted here. A similar discrepancy between what is effectively the predicted mass loss rate of a B star and its "observed" value has been noted elsewhere (Kudritzki et al. 1991; Drew et al. 1994).

Table 1. B star parameters.

No.	Name	Spectral Type	$v \sin i$ (km s^{-1})	M ($M_\odot$)	R ($R_\odot$)	T$_{eff}$ (10^3K)	$\log_{10}\dot{M}$ (M$_\odot$ yr^{-1})	v_∞ (km s^{-1})	r_I (R_*)	v_I (km s^{-1})	r_S (R_*)	v_{edge} (km s^{-1})	T_S (10^6K) $\xi=1$ ($\xi=0.25$)	L_X/L_{Bol} (10^{-7}) $\xi=1$ ($\xi=0.25$)
(a) spectral type sequence														
1		B0.5		14.3	8.2	29.2	-7.8	1650			2.40	1130	3.2(8.4)	6.0(19.0)
2		B1		10.4	6.8	26.9	-8.3	1570			1.76	870	2.2(5.8)	2.0(7.0)
3		B1.5		13.6	6.3	25.7	-8.5	1890			1.22	570	2.4(5.7)	1.5(6.0)
4		B2		10.3	6.0	22.8	-9.0	1690			1.24	540	1.5(3.6)	0.4(2.0)
5		B2.5		10.4	5.2	20.4	-9.5	1830			1.19	510	0.9(2.1)	0.1(0.5)
6		B3		8.8	5.1	18.5	-9.9	1700	2.15	1320	1.18	460	0.7(1.5)	0.03(0.2)
7		B4		6.8	4.7	16.3	-10.4	1560	1.11	340	1.20	440	0.4(0.9)	0.005(0.04)
(b) individual stars from Snow (1981, 1982)														
8	25Ori	B1Vn	300	15.0	8.0	22.5	-8.65	1760			1.65	920	1.4(3.4)	0.8(2.0)
9	59Cyg	B1.5Ve	375	14.0	7.5	20.7	-9.81	1760	1.24	620	1.80	1000	0.4(0.9)	0.002(0.02)
10	HD28947	B1.5Ve	340	14.0	7.5	20.7	-9.11	1760			1.69	940	0.8(2.1)	0.1(0.6)
11	δCru	B2IV	175	13.0	7.0	22.1	-10.40	1760	1.05	220	1.05	210	0.5(1.1)	0.001(0.01)
12	ζCen	B2.5IV	225	12.0	6.8	17.4	-10.40	1720	1.06	240	1.11	350	0.4(0.8)	0.002(0.01)
13	γLup	B2.5IV	270	13.0	7.0	22.1	-10.02	1760	1.11	360	1.07	250	0.7(1.5)	0.008(0.04)
14	ωCMa	B2.5Ve	110	13.0	7.0	19.3	-9.86	1760	1.24	610	1.91	1050	0.3(0.9)	0.001(0.03)
15	νCyg	B2.5Ve	255	13.0	7.0	18.4	-10.20	1760	1.07	280	1.23	550	0.3(0.8)	0.001(0.01)
16	48Lib	B3IVpe	405	7.0	5.2	15.7	-10.17	1500	1.24	520	1.14	350	0.5(1.2)	0.02(0.1)
17	αEri	B3Vpe	250	11.0	5.9	14.4	-9.88	1770	1.49	930	1.22	540	0.5(1.3)	0.03(0.3)
18	ψPer	B5Ve	375	7.0	5.2	17.2	-10.12	1500	1.28	570	1.28	515	0.4(1.1)	0.001(0.08)

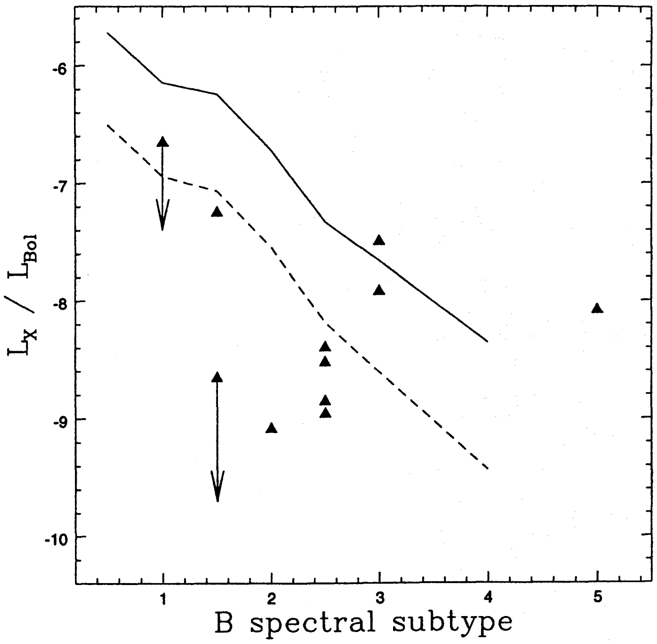

Fig. 2. Predicted X-ray luminosities vs. spectral type for the individual stars. The two lines show the trend followed by the representative stars - the solid line was calculated with $\xi = 0.25$, whereas the dashed line was calculated with $\xi = 0.25$ *and* a mass loss rate of a third of that derived using Garmany et al. 's (1981) relationship. The symbols represent the individual stars' emission calculated with $\xi = 0.25$. The two arrows indicate the typical shifts in emission when $\xi = 1.0$; one for high shock temperature, and one for low shock temperature

Is it likely that the decoupling mechanism is ion-stripping? The ion stripping radius r_I is calculated by integrating Eq. (5). This radius also defines the velocity v_I at which the ion stripping begins. It is calculated using the velocity law in Eq. (1) with $\beta = 0.8$. Values obtained for r_I and v_I are set out in columns 10 and 11 of Table 1. Applying the purely dynamic argument, the ion stripping radius calculated according to Eq. (4) is somewhat larger than that derived from Eq. (5). This shows the significant effect of frictional heating. The temperatures attained in the plasma at decoupling are $\sim 2-4T_{\rm eff}$, similar to Springmann & Pauldrach's (1992) result. This falls far short of the level required for consistency with the observed X-ray emission. Where, in Table 1, there is no entry for r_I and v_I, the stated stellar parameters (M_* , R_*, $T_{\rm eff}$) do not allow ion stripping at a finite radius.

On contrasting the velocities v_I with the observed maximum expansion velocities (Grady et al. 1987), displayed in column 13, it can be seen that the former are, in general, greater than the latter in the representative B star sample (nos. 1-7). Again this can be seen as a direct consequence of inflated mass loss rates. The comparison with the sample derived from Snow's data (nos.8-18) is more favourable. In most instances, the agreement is to within 150 km s^{-1} (Grady et al. estimate the error in the maximum velocities to be $\pm$100 km s^{-1}). If anything, the calculated decoupling velocities are inclined to be smaller than the measured v_{edge}, and there are a couple of clearly discrepant cases (59 Cyg and ω CMa). On its own, the similarity between the observed and derived edge velocities would support the view that ion-stripping is responsible for the decoupling.

4. Analytic streamline modelling

A semi-analytic model of flows around Be stars has been presented by Bjorkman & Cassinelli (1991, 1993). Their treatment assumes wind properties as numerically evaluated by Friend & Abbott (1986) for the outflow in the equatorial plane of a rotating star. Bjorkman & Cassinelli's analysis is repeated here, with the difference that decoupling between the plasma and the stellar radiation field is taken into account. If the driven metal ions are either stripped out of the gas, or are ionized away by shocks at some radius, there the radiative acceleration applied to the bulk of the outflow ceases, inhibiting further increase of the wind speed. For radii greater than the decoupling radius the β velocity law is replaced by a constant $v(r) = v_{dec} = v(r_{dec})$, ie.

$$v = \begin{cases} v_\infty(1 - R_*/r)^\beta & \text{before decoupling} \\ v_{dec} = v_\infty(1 - R_*/r_{dec})^\beta & \text{after decoupling.} \end{cases} \tag{12}$$

With this velocity prescription, the streamlines may now be calculated and compared with flow in which no decoupling occurs.

The following parameters are used for the central star: $M_* = 13M_\odot$, $R_* = 7R_\odot$, $T_{\rm eff} = 22100$K and $\dot{M} = 10^{-9.9} M_\odot\, {\rm yr}^{-1}$. Also the rotation is set in the first instance at 50% of the critical rotation rate. Streamlines can be determined quite straightforwardly once the gas, has left the star's surface. As an example of the wind compression, Fig. 3 shows the effect for the representative Be star with no decoupling (the standard Bjorkman & Cassinelli 1993 model).

We calculate the flow around the standard star for different values of the decoupling radius which is set to a constant value for all directions of flow (in practice this radius depends on polar angle, we find for the standard star, the ion stripping radii is $1.1R_*$ at the pole and $1.22R_*$ at the equator). Outside the decoupling radius, the radial velocity remains constant. This enables the wind to be focused more easily onto the equatorial plane than an accelerating wind. The result is that the density enhancement of the equatorial WCD compared to the poles increases over the fully-coupled wind model. The effect on the streamlines of changes in the decoupling radius is illustrated in Figs. 4 & 5. The decoupling radius has been varied from $2.0R_*$ down to $1.1R_*$. As can be seen, when the decoupling radius is close to the star there is an enormous difference in the resulting flow over a similar calculation with no decoupling. Inspection of Table 1 indicates that decoupling radii of $1.1R_*$–$1.3R_*$ are appropriate to early B stars.

A quantitative way in which to analyze the effect of decoupling on the WCD is to examine the ratio of momentum input rate normal to the plane of the disc, with and without decoupling $\mathscr{M}_D/\mathscr{M}$. This is achieved by summing the product of mass loss rate and normal velocity over all equator crossing streamlines. The ratio indicates how much extra momentum is input normal to the disc – it is this which defines how much

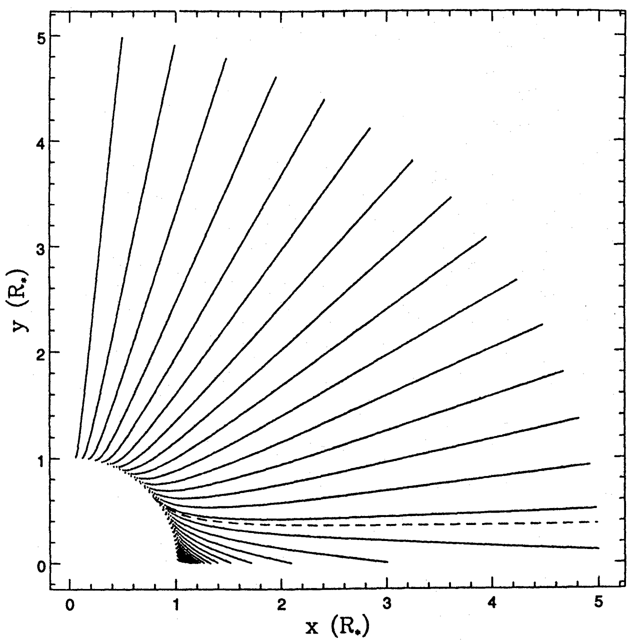

Fig. 3. Streamlines of the wind from the representative Be star. v_{rot}/v_{crit} = 0.5. Note that streamlines cross the equator leading to a wind compressed disc. In this simulation, decoupling has not been included. The dotted line marks the streamline which separates the flow into that which will approach the equatorial plane, and that which will not

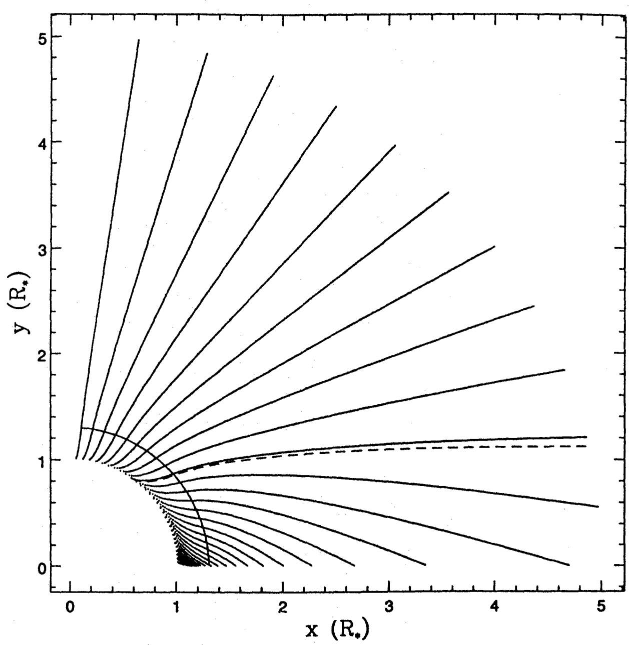

Fig. 4. Streamlines for the representative Be star. v_{rot}/v_{crit} = 0.5. The solid line marks the radius at which decoupling occurs, set here to be $1.3R_*$

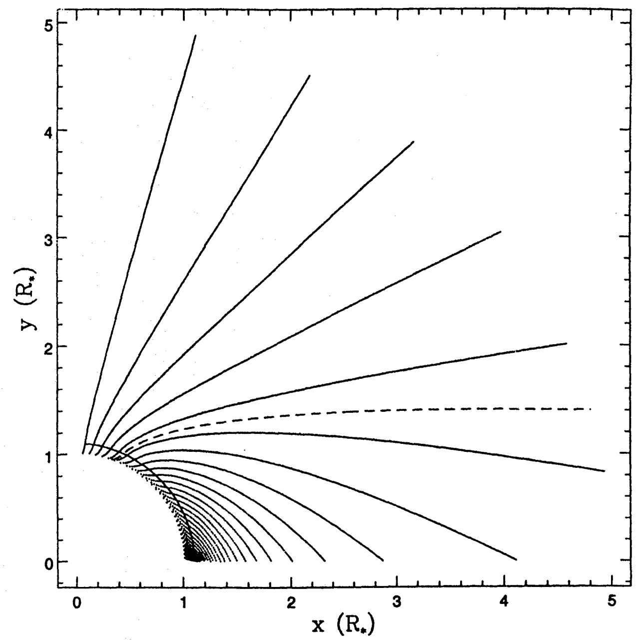

Fig. 5. As in Fig. 4 except the decoupling radius is $1.1R_*$

Table 2. Momentum input rate normal to the equatorial plane. The mass loss rate was set to $10^{-9.9}$M$_\odot$ yr^{-1}

r_{dec} (R_*)	v_{rot}/v_{crit}	$\mathcal{M}_D/\mathcal{M}$ ($r > R_*$)	$\mathcal{M}_D/\mathcal{M}$ ($r > r_{dec}$)
2.0	0.5	1.05	1.50
1.9	"	1.06	1.52
1.8	"	1.08	1.59
1.7	"	1.11	1.68
1.6	"	1.15	1.79
1.5	"	1.22	1.88
1.4	"	1.32	1.87
1.3	"	1.50	2.03
1.2	"	1.82	2.07
1.1	"	2.50	2.50
1.2	0.4	7.75	7.75
"	0.5	1.82	2.07
"	0.6	1.28	2.06
"	0.7	1.13	2.16
"	0.8	1.07	2.10
"	0.9	1.03	2.23

compression is produced and hence provides a pointer to the relative equatorial densities in the two models. It is also radius dependent – upstream of decoupling, the two flows are identical. However, the post-decoupling flow is very different to the flow in the equivalent calculation with no decoupling (see Figs. 3 and 4 & 5). Thus, two ratios of normal momentum input rate are calculated. One, $\mathcal{M}_D/\mathcal{M}(r > R_*)$ considers the whole disc, indicating how much more effective the wind is in keeping the disc confined when ion stripping is included, compared to the standard Bjorkman & Cassinelli model. The second $\mathcal{M}_D/\mathcal{M}(r > r_{dec})$, only considers the flow outside the decoupling surface. This second ratio will indicate how much effect the mechanism has on the disc at radii beyond the decoupling radius; ie. it is a measure of the difference in the effectiveness of the more extended material in confining the disc, between models with and without the effect. Table 2 shows these two ratios for different values of the decoupling radius.

We now set the decoupling radius to be $1.2R_*$ and illustrate the effect of changing the rotational velocity of the star. The ratios in Table 2 show that for low rotation, the extra momentum input normal to the disc will increase the equatorial density substantially; for $v_{rot}/v_{crit} = 0.5$ there is an increase of 80% the total normal momentum input rate. For lower rotation, this ratio increases dramatically - indeed the decoupling of the wind leads to a lower threshold of v_{rot}/v_{crit} for disc formation. We find that for the stellar parameters used above the rotational threshold for disc formation with ion stripping is $v_{rot}/v_{crit} = 0.25$, whilst in fully coupled flow $v_{rot}/v_{crit} = 0.38$.

Hence, the addition of more material to the disc is qualitatively more important in the slower rotating stars, making discs denser and accordingly more readily detectable. As the rotation increases, much more of the input momentum (and mass) is deposited in the equatorial plane very close to the star, so that little extra momentum is added after the decoupling radius. For high rotation the extra confinement may not be sufficient to bring the theory of WCD into line with the estimates derived from observation, if indeed an order of magnitude increase is required.

In the cases of practical interest (see Table 1) we have found that the normal momentum added in the decoupled flow is at least twice that in fully coupled winds (Table 2).

5. Discussion

The streamlines generated from the model with and without decoupling are striking in their difference. Truncation of the velocity profile at relatively low velocities leads to a higher fraction of mass loss from the star being focussed onto the equatorial plane. The decoupled material flows into the disc much less obliquely, enabling it to apply larger compressive forces as seen in Sect. 4. It is particularly effective at the lower rotations where it may be the dominant cause of compression. Indeed, it has been shown that wind compressed discs can be expected to form at lower rotational velocities when decoupling is taken into account.

However, equator to pole density ratios have *not* been calculated using Bjorkman & Cassinelli's (1993) prescription. This is because the description of the compression disc in their work is vastly different from that found in Owocki et al. 's (1994) numerical simulations. Direct numerical simulation of a wind with and without decoupling (Porter & Whitehurst, in preparation) will attempt to clarify the disc structure. Thus far we have seen that decoupling of radiation and outflow must lead to distinctly higher compression ratios.

The observable effect, that initially helped draw attention to the possibility of decoupling following on termination of the wind's cool phase, is that the maximum absorption blueshift may imply a maximum outflow velocity well below v_∞ calculated from Eq. 2 (Friend & Abbott 1986). The difference is a factor of ~2–4 for the near-MS B-stars of interest here. Strictly, the UV line profiles should be modelled in a way that recognizes the wind density profile for a cut-off velocity law is not so steeply declining as in the case that the observed maximum velocity is v_∞ in its usual sense. In practice, this distinction has not been made, but it does not produce large errors. To verify this we have emulated Snow's method of mass loss rate determination by experimenting numerically with fitting line profiles calculated under the assumption of fully coupled flow to line profiles derived for decoupled outflow. We find that the discrepancies in the mass loss rate caused by this to be no worse than $\sim 20\%$. As pointed out by Snow, the main uncertainty lies in the ionization corrections.

We have considered two mechanisms that both lead to heating of the wind and, in the case of wind shocking – over-ionization also, that in turn produce the dynamical decoupling of the outflow from the driving radiation. We have also used a range of observational and semi-empirical data on early B-stars (including Snow's 1981 mass loss rates) to assess their relative merits. There is still much to do to improve the quality of the database all round - more X-ray observations of B stars are clearly desirable, and there is scope to look again at UV mass loss rate determinations. We have compared data available with a simple prescription for an upper-limit to the X-ray emission in the case that just a single strong shock, terminating the cool-phase of the outflow, dominates the emission. Surprisingly, perhaps, we find no evidence that this limit is seriously violated. We also find that the decline in X-ray emission with increasing spectral sub-type between B0 and B4 apparent in the ROSAT data of Cassinelli et al. (1994) is tracked by our simple prescription. However, uncertainties in the measurement of stellar and wind parameters remain large enough that these results are suggestive rather than final.

Whilst the mechanism of ion-stripping has aesthetic appeal by virtue of its straightforwardly deterministic nature, there is the problem that it fails, on its own, to provide temperatures high enough to fit in with analyses of X-ray data. It has emerged here that decoupling radii calculated according to the ion-stripping model are usually of the right order to fit in with estimates derived from observation. In order to save the ion-stripping hypothesis as the cause of the decoupling it is necessary to identify an alternative source of the X-ray emission from B stars. We have shown that the momentum input normal to the disc does increase, in part due to higher normal velocities (an increase of ~ 2 over that standard fully coupled model). These velocities generate the observed shock temperatures of $3\times10^6 - 4\times10^6$K (e.g. Cassinelli et al. 1994). So although ion-stripping may not be able to produce the required X-ray emission directly, it may do so indirectly via the shock bounding the WCD.

The fact remains that our prescription for the X-ray emission invoking shock decoupling adequately matches the limited observational data presently available. The underlying assumptions of this treatment have the virtue of simplicity. It is yet to be worked out whether or not the properties of shocks bounding WCD would lead to a similar predicted dependence of L_X/L_{Bol}

on spectral type. Such a calculation could usefully descriminate between the two mechanisms. Regardless of which mechanism leads to decoupling, its result is certain to be an enhancement of the Bjorkman & Cassinelli effect.

Acknowledgements. JMP acknowledges financial support from a SERC studentship, and JED from a SERC Advanced Fellowship.

References

Abbott, D. C. 1982, ApJ, 259, 282
Abbott, D. C., Beiging, J. H., Churchwell, E., 1981, ApJ, 250, 645
Abbott, D. C., Beiging, J. H., Churchwell, E., 1984, ApJ, 280, 671
Abbott, M. J., Friend, D. B., 1989, ApJ, 345, 505
Ando, H., 1991, in *Rapid Variability of OB stars: Nature and Diagnostic Value*, ed. D. Baade. ESO Conference and Workshop Proceedings No. 36, p303
Batten, A. H., Fletcher, J. M., Mann, P. J., 1978, Pub. Dom. Astrophys. Obs., 15, No. 5
Bjorkman, J. E., Cassinelli, J.P., 1990, in *Angular Momentum and Mass Loss from Hot Stars*, eds. L. A. Willson & G. H. Bowen (Dordercht: Kluwer Academic Publishers) 185
Bjorkman, J. E., Cassinelli, J.P., 1993, ApJ, 409, 429
Cassinelli, J. P., Cohen, D. H., MacFarlane, J. J., Sanders, W. T., Welsh, B. Y., 1994, ApJ, 421, 705
Cassinelli, J. P., Swank, J. H., 1983, ApJ, 271, 681
Cassinelli, J. P., Waldron, W. L., Sanders, W. T., Harndon, F. R., Rosner, R., Vaiana, G. S., 1981, ApJ, 250, 677
Castor, J. I., 1987, in *Instabilities in Luminous Early-Type Stars*, eds. H. J. G. L. M. Lamers & C. W. H. de Loore, D. Reidel, The Netherlands, p159
Castor, J. I., Abbott, D. C., Klein, R. I., 1975, ApJ, 195, 157
Castor, J. I., Lamers, H. J. G. L. M., 1979, ApJS, 39, 481
Chlebowski, T., Harnden, F., Sciortino, S., 1989, ApJ, 341, 427
Code, A. D., Davis, J., Bless, R. C., Hanbury-Brown, R., 1976, ApJ, 203, 417
Coté J., Waters, L. B. F. M., 1987, A&A, 176, 93
Dreicer, H., 1959, Phys. Rev., 115, 238
Dreicer, H., 1960, Phys. Rev., 117, 329
Drew, J. E., Denby, M., Hoare, M.G. 1994, MNRAS, 266, 917
Friend, D. B., Abbott, D. C., 1986, ApJ, 311, 701
Gaetz, T. J., Salpeter, E. E., 1983 ApJS 52, 155
Garmany, C. D., Olson, G. L., Conti, P. S., Van Steenberg, M. E., 1981, ApJ, 250, 660
Gayley, K. G., Owocki, S. P., 1994, ApJ, submitted
Grady, C. A., Bjorkman, K. S., Snow, T. P., 1987, ApJ, 320, 376
Harnden, F. R. Jr., Branduardi, G., Elvis, M., Gorenstein, P., Grindlay, J., Pye, J. P., Rosner, R., Topka, K., Vaiana, G. S., 1979, ApJL, 234, L51
Kallman, T., 1980, Ph.D thesis, University of Colorado
Krolik, J. H., Raymond, J. C., 1985, ApJ, 298, 660
Kudritzki, R. P., Pauldrach, A., Puls, J., Abbott, D. C., 1989, A&A, 219, 205
Kudritzki, R. P., Puls, J., Gabler, R., Schmitt, J. H. M. M., 1991, in *"Extreme Ultraviolet Astronomy"*, eds. R. F. Malina & S. Bowyer, Pergamon, USA, p130
Lucy , L. B., 1982, ApJ, 255, 286
Lucy , L. B., Solomon, P. M., 1970, ApJ, 159, 879
MacGregor, K. B., Hartmann, L., Raymond, J. C., 1979, ApJ, 231, 514
Mauche, C. W., Raymond, J. C., 1987, ApJ, 323, 690
Owocki, S. P., 1991, in *"Stellar Atmospheres: Beyond Classical Models"*, eds. L. Crivellari, I. Hubeny & D. G. Hummer, p. 337
Owocki, S.P., Castor, J.I., Rybicki G.B., 1988, ApJ, 335, 914
Owocki, S. P., Cranmer, S. R., Blondin, J. M., 1994, ApJ, 424, 887
Owocki, S. P., Rybicki, G. B., 1984, ApJ, 284, 337
Pauldrach, A., Puls, J., Kudritzki, R.P. 1986, A&A, 164, 86
Pockert, R., Marlborough, J.M., 1978, ApJ, 220, 940
Popper, D. M., 1974, ApJ, 188, 559
Popper, D. M., 1978, ApJL, 220, L11
Raymond, J. C., Cox, D. P., Smith, B. W. 1976, ApJ, 204, 290
Schmidt-Kaler, Th., in *Landolt Börnstein New Series*, Vol 2b, eds. K. Schaifers & H. H. Voigt, Springer-Verlag, Berlin
Sciortino, S., Vaiana, G. S., Harnden, F. R. et al., 1990, ApJ, 361, 621
Snow, T. P., 1981, ApJ, 251, 139
Snow, T. P., 1982, ApJL, 253, L39
Snow, T. P., Morton, 1976, ApJS, 32, 429
Springmann, U. W. E., Pauldrach, A. W. A., 1992, A&A, 262, 515
Underhill, A. B., Divan, L., Prévot-Burnichon, M.-L., Doazan, V., 1979, MNRAS, 189, 601
Underhill, A. B., Doazan, V., (eds.) *B Stars with and without Emission lines*, (NASA SP-456), pp. 34-38, 59-62
Waldron, W., L., 1984, ApJ, 282, 256
Waters, L. B. F. M., Cotè J., Lamers, H. J. G. L. M., 1987, A&A, 185, 206
Willson, L. A., 1986, PASP, 98, 370

This article was processed by the author using Springer-Verlag LaTeX A&A style file version 3.